

TWO-DIMENSIONAL BEHAVIOR OF THE SUBLATTICE MAGNETIZATION IN THREE DIMENSIONAL ISING ANTIFERROMAGNETS

O. PETRACIC, CH. BINEK AND W. KLEEMANN

*Laboratorium für Angewandte Physik, Gerhard-Mercator-Universität Duisburg,
D-47048 Duisburg, Germany*

A three-dimensional layered Ising-Antiferromagnet with a ferromagnetic intra-layer coupling to z neighbors, $zJ > 0$, and an antiferromagnetic interlayer coupling to z' neighbors, $z'J' < 0$, is investigated by Monte Carlo simulations on a hexagonal lattice. The physical nature of the anomalous temperature behavior of the sublattice magnetizations, which is found for certain values of $r = zJ/z'J'$ and z' in magnetic fields is explained in terms of successive phase transitions. They take place on the ferromagnetic 2-dimensional spin-down sublattice at $T \approx T_c^{2d}$, smeared by a finite stabilizing molecular field, and on both antiferromagnetically coupled sublattices at $T_c^{3d} > T_c^{2d}$.

1 Introduction

Anisotropic three-dimensional antiferromagnets (AFs) are still an interesting subject of theoretical investigations. There exist many investigations e.g. on their magnetic phase diagram within the framework of Ising or anisotropic Heisenberg models.¹⁻¹¹ It is found, that layered Ising AFs with two competing interaction parameters (Fig. 1) may exhibit two rather different phase diagrams (Fig. 2) depending only on two parameters, the ratio $r = zJ/z'J'$ and z' ,⁹ where J and J' are the coupling constants of the intra-layer and of the inter-layer exchange, respectively; z and z' are the coordination numbers of the couplings. The Ising Hamiltonian is of the form:

$$\mathcal{H} = -J \sum_{\langle i,j \rangle} S_i S_j - J' \sum_{\langle i,j \rangle} S_i S_j - H \sum_i S_i, \quad (1)$$

where H is the applied magnetic field acting on all spins S_i , with $S_i = \pm 1$. The two kinds of phase diagrams are continuously transformed into one another by changing the crucial parameters r and z' . For large values of $|r|$, i.e. $|r| > 0.6$,³ and small values for z' , i.e. $z' < 10$,⁹ the FeCl_2 -like phase diagram¹² is found (Fig. 2 (b)), whereas for low values of $|r|$ and large values for z' the case (b) in Fig. 2 appears. This second case is characterized by three interesting features. On the one hand, a possible decoupling of the tricritical point (TCP) into a critical endpoint (CEP) and a bicritical endpoint (BCE)

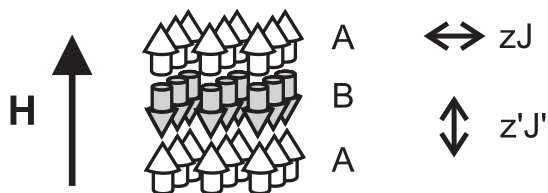


Figure 1. Schematic drawing of a layered 3-dimensional antiferromagnet with a ferromagnetic coupling in the layers, $J_{A-A} = J_{B-B} = zJ$, and an antiferromagnetic coupling between adjacent layers, $J_{A-B} = J_{B-A} = z'J'$. The magnetic field, H , is applied along the antiferromagnetic stacking direction.

is encountered. From previous investigations it follows, that this decoupling is only observed in mean field calculations,²⁻⁹ while in Monte Carlo simulations only one multicritical point is found.¹⁰ On the other hand, the second-order phase line has a balloon-like shape and extends even above the limiting field value H_{c0} (spin-flip field at $T = 0$). This means, that for some fixed field values $H > H_{c0}$ it is possible to cross this phase line twice with increasing temperature T . Furthermore, above and below the critical line anomaly lines are found, where the magnetization exhibits an additional inflection point and the specific heat shows an additional broad maximum.^{9,10}

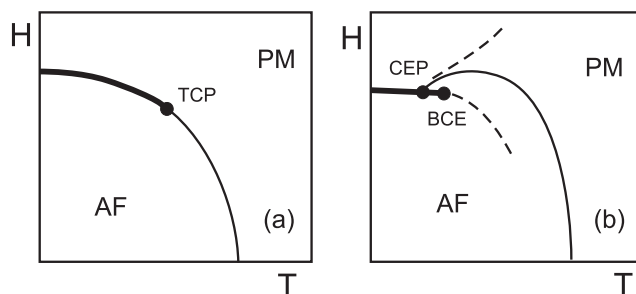


Figure 2. Schematic magnetic phase diagrams of 3-dimensional layered Ising AFs (see Figure 1) choosing (a) $|r|$ large and z' small (e.g. $|r| = 1.0$ and $z' = 4$), and (b) vice versa (e.g. $|r| = 0.4$ and $z' = 20$). Bold, thin and broken lines refer to first- and second-order phase transitions and anomalies, respectively. Transitions occur between the antiferromagnetic (AF) and paramagnetic (PM) phase. TCP, CEP, BCE denote tricritical, critical end- and bicritical endpoints, respectively.

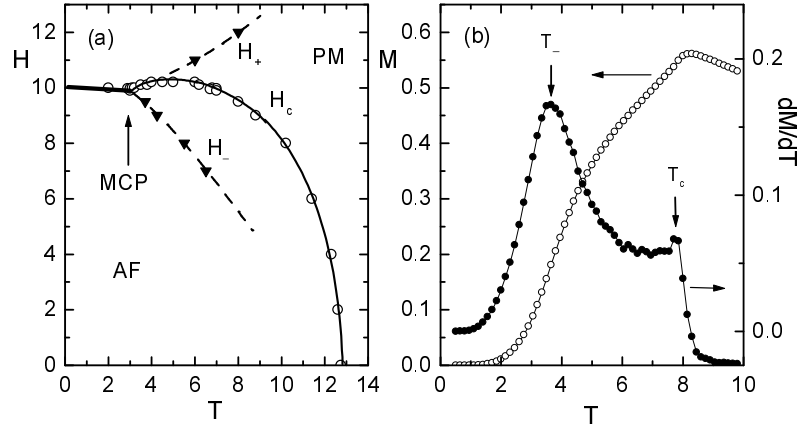


Figure 3. (a) H - T phase diagram of a 3-dimensional Ising antiferromagnet on a hexagonal lattice ($24 \times 24 \times 18$) with coupling constants $zJ = 6 \cdot 0.7$ and $z'J' = -20 \cdot 0.5$ ($k_B = 1$). Periodic boundary conditions for all axes were used. For $T < T_{MCP} \approx 3$ the phase transition is discontinuous, while for $T > T_{MCP}$ a second-order phase transition occurs at the line $H_c(T)$. The broken lines denoted as H_- and H_+ are the anomaly lines. (b) Calculated magnetization M (open circles) and its derivative dM/dT (full circles) vs temperature T in a field $H = 9.5$.

2 Comparison between theory and experiment

Fig. 3 (a) shows the H - T phase diagram of a 3-dimensional layered Ising AF obtained from Monte-Carlo simulations on a hexagonal lattice with periodic boundary conditions. All quantities like T , H , J and J' are considered to be dimensionless. For the simulation the Metropolis algorithm was used with $k_B = 1$. The parameters z, z', J, J' are chosen such as to reproduce case (b) of Fig. 2. One observes only one multicritical point (MCP), where a first-order phase line ($T < T_{MCP}$) and a second order phase line, $H_c(T)$ meet, and where the two anomaly lines, H_- and H_+ , originate.

Fig. 3 (b) shows one magnetization curve, referring to the phase diagram of Fig. 3 (a), as a function of temperature for $H = 9.5$ and its derivative, dM/dT . The magnetization is defined to be $M = \sum_i S_i/N$, where N is the number of lattice sites. M vs T clearly shows an anomalous curvature for $T < T_c$, which manifests itself in the derivative as an additional broad maximum.

The phase diagram shown in Fig. 3 (a) resembles that of FeBr_2 , an insulating uniaxial antiferromagnet with $T_N = 14.2$ K^{13–16} (Fig. 4). Both

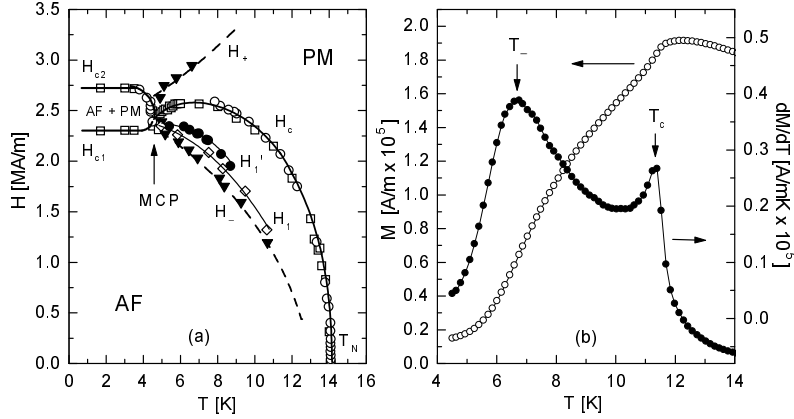


Figure 4. (a) H - T phase diagram of FeBr_2 , where H is the applied axial magnetic field. The lines H_c , H_{c1} , H_{c2} , H_- and H_+ were obtained by magnetization or susceptibility measurements. H_1 and H'_1 denote the positions of the spikes found by specific heat (open diamonds) (Ref. 14) and off-axis magnetization measurements vs temperature (solid circles), respectively. (b) Magnetization M vs temperature T and its derivative for a field $H = 2.07$ MA/m (field parallel to the c -axis). The phase lines H_1 or H'_1 are not seen in this configuration (see Ref. 16). The broad peak at $T_- = T(H_-)$ is due to strong non-critical fluctuations (Ref. 13).

in Fig. 3 and Fig. 4 lines of non-critical fluctuations (or anomaly lines) do appear. In this article the attention is focused on these non-critical fluctuations at $T_- = T(H_-)$. Although this phenomenon is well investigated both in experiments^{13,15,16} on FeBr_2 and in theory⁸⁻¹⁰ no clear explanation for the occurrence of these fluctuations yet exists. Especially one wonders, how it is possible that two completely different types of phase diagrams are found by varying only two parameters, r and z' .

3 Non-critical fluctuations

In order to gain insight into the origin of the non-critical fluctuations at $H_-(T)$, we performed systematic Monte Carlo simulations of the sublattice magnetizations with the same parameters as in Fig. 3, $zJ = 4.2$ and $z'J' = -10.0$. The exchange constants and especially the number of coupled neighbours are comparable to those in FeBr_2 .¹⁷ However, here we used only two exchange couplings. The different intra-planar exchange parameters found in FeBr_2 were absorbed in one ferromagnetic effective intra-planar cou-

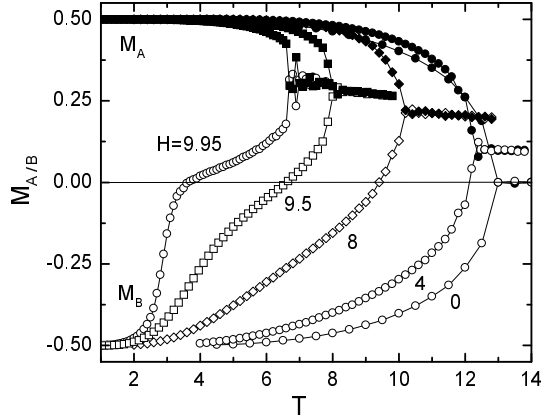


Figure 5. Sublattice magnetization of an Ising AF with an hexagonal lattice ($24 \times 24 \times 18$) and $zJ = 6 \cdot 0.7$ and $z'J' = -20 \cdot 0.5$ ($k_B = 1$). For low values of H the sublattice magnetization M_A and M_B are as expected for an uniaxial antiferromagnet. By increasing the field value the sublattice magnetizations become strongly asymmetric.

pling constant. Fig. 5 shows the temperature dependences of the sublattice magnetizations, M_A and M_B (see Fig. 1), for $H = 0, 4, 8, 9.5$ and 9.95 , respectively. While M_A (parallel) and M_B (antiparallel to \mathbf{H}) are symmetric for zero field, $M_A(T) = -M_B(T)$, they become more and more inequivalent with increasing field. For fields coming close to the spin-flip one, $H_{c0} = 10$, anomalous bumps appear at $T \approx T_-$ in $M_B(T)$, whereas $M_A(T)$ is virtually constant up to that temperature. Obviously all of the non-critical fluctuations observed at $T \approx T_-$ happen to occur merely on the B-sublattice. In other words, these fluctuations are essentially constrained to 2-dimensional (2d) layers separated by magnetically saturated up-spin layers of the A-sublattice. It is, hence, tempting to compare the B-sublattice with an ensemble of 2d ferromagnets (FMs) with the same intra-layer parameters, $zJ > 0$, but subjected to a field $H_{eff} = H - H_{c0}$, where H is the field applied to the corresponding 3d AF.

Fig. 6 shows the sublattice magnetization curves for $H = 9.5$ and 9.95 as before and the magnetization curves of a 2d FM with $zJ = 4.2$ in fields $H_{eff} = -0.5$ and -0.05 , respectively. One observes, that the magnetization curve of the 2d FM fits well with the spin-down sublattice magnetization M_B up to the inflection point at T_- (arrows). It seems, that the magnetization of the spin-down sublattice behaves like a 2d FM in an effective mean field,

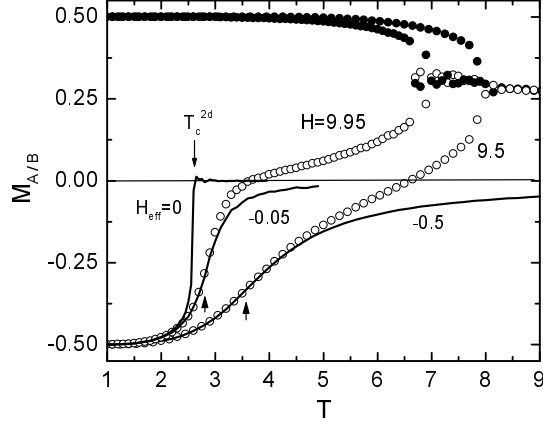


Figure 6. Two examples of sublattice magnetizations (circles) of the model as in Fig. 5 ($H_{c0} = -z'J' = 10.0$) and in addition magnetization curves of a 2d FM (solid lines) with $zJ = 6 \cdot 0.7$ in fields $H_{eff} = H - H_{c0} = 0, -0.05,$ and $-0.5,$ respectively. Arrows denote the inflection point, which is associated with T_- .

which is the sum of the external applied field H and the field, produced by the fully magnetized spin-up sublattice (A-sublattice), $H_{eff} = H + H_A$. Since M_A is completely magnetized, $H_A = z'J' = -H_{c0}$, one has $H_{eff} = H - H_{c0}$.

If the effective field H_{eff} becomes zero ($H_{eff} = 0 \Leftrightarrow H = H_{c0}$) we have the case of a 2d FM in zero field, which undergoes a phase transition at T_c^{2d} and becomes paramagnetic for $T > T_c^{2d}$ (see Fig. 6). Although this case cannot be obtained here, because of the spin-flip occurring in the range $H_{MCP} < H < H_{c0}$, the anomaly temperatures T_- can be associated with the points of inflection of the $M(H_{eff})$ vs T curves of the 2d Ising FM (arrows in Fig. 6). Therefore one can conclude, that the anomaly of M_B signifies the thermal destruction of 2d ferromagnetic order on the quasi-decoupled B-sublattice layers, which precedes the global 3d phase transition of both sublattices. In other words, the anomaly we find in the magnetization is due to the finite temperature range lying between T_c^{2d} and T_c^{3d} . If this splitting is reduced by increasing the intra-planar ferromagnetic interaction and thus increasing the 2d transition temperature, the anomaly decreases and vice versa.

4 Conclusion

The occurrence of anomalies, which are observed in certain 3d Ising AFs is due to the separation of the smeared 2d phase transition on one sublattice from the 3d global phase transition of both sublattices. This is typical of antiferromagnets, whose inter-planar antiferromagnetic coupling is strong compared with the intra-planar exchange ($|r| = |zJ/z'J'| < 0.6$)³. A high value of the inter-planar exchange gives rise to a high value of the spin-flip field $H_{c0} = -z'J'$. This results in a strong stabilization of the spin-up sublattice, which acts only as a mean-field $H_{MF} = z'J'$ on the spin-down sublattice. Hence, the spin-down sublattice behaves like a 2d FM in an effective field $H_{eff} = H + H_{MF}$. The quality of the mean-field approximation crucially depends on a high coordination number z' , which is needed for integrating out thermal spin-fluctuations.

Acknowledgments

We would like to thank M. Acharyya and U. Nowak for helpful discussions and the Deutsche Forschungsgemeinschaft (Graduiertenkolleg "Struktur und Dynamik heterogener Systeme") for financial support.

References

1. F. Harbus and H.E. Stanley, *Phys. Rev. B* **8**, 1141 (1973).
2. A.R. Fert, J. Gelard, and P. Carrara, *J. Phys. Chem. Sol.* **35**, 261 (1974).
3. J.M. Kincaid and E.G.D. Cohen, *Phys. Rep. C* **22**, 57 (1975).
4. H.J. Herrmann, E.B. Rasmussen, and D.P. Landau, *J. Appl. Phys.* **53**, 7994 (1982).
5. I. Vilfan and S. Galam, *Phys. Rev. B* **34**, 6428 (1986).
6. Y.L. Wang and J.D. Kimel, *J. Appl. Phys.* **69**, 6176 (1991).
7. H.J. Herrmann and D.P. Landau, *Phys. Rev. B* **48**, 239 (1993).
8. W. Selke and S. Dasgupta, *J. Magn. Magn. Mater.* **147**, L245 (1995).
9. W. Selke, *Z. Phys. B* **101**, 145 (1996).
10. M. Pleimling and W. Selke, *Phys. Rev. B* **56**, 8855 (1997).
11. M. Pleimling, *Eur. Phys. J. B* (in print, cond-mat/9902237).
12. C. Vettier, H.L. Alberts, and D. Bloch, *Phys. Rev. Lett.* **31**, 1414 (1973).
13. M.M.P. de Azevedo, Ch. Binek, J. Kushauer, W. Kleemann, and D. Bertrand, *J. Magn. Magn. Mater.* **140-144**, 1557 (1995).
14. H. Aruga Katori, K. Katsumata, and M. Katori, *Phys. Rev. B* **54**, R9620 (1996).

15. O. Petracic, Ch. Binek, and W. Kleemann, *J. Appl. Phys.* **81**, 4145 (1997).
16. O. Petracic, Ch. Binek, and W. Kleemann, U. Neuhausen, and H. Lueken, *Phys. Rev. B* **57**, R11051 (1998).
17. W.B. Yelon, C. Vettier, *J. Phys, C* **8**, 2760 (1975).